Intermetallics 40 (2013) 36–44

Contents lists available at SciVerse ScienceDirect

Intermetallics

journal homepage: www.elsevier.com/locate/intermet

In situ formation of various intermetallic particles in Al–Ti–X(Cu, Mg) systems during friction stir processing

Q. Zhang [a,b], B.L. Xiao [a], Z.Y. Ma [a,*]

[a] Shenyang National Laboratory for Materials Science, Institute of Metal Research, Chinese Academy of Sciences, 72 Wenhua Road, Shenyang 110016, China
[b] University of Science and Technology of China, 96 Jinzhai Road, Hefei 230026, China

ARTICLE INFO

Article history:
Received 13 March 2013
Accepted 4 April 2013
Available online 3 May 2013

Keywords:
A. Composites
A. Aluminides, miscellaneous
B. Dispersion strengthening
B. Phase identification
C. Reaction synthesis

ABSTRACT

In situ Al composites reinforced by various intermetallic particles were fabricated from Al–Ti–X(Cu, Mg) systems by hot pressing, forging and subsequent 4-pass friction stir processing (FSP). The formation of various intermetallic particles during FSP and the tensile properties of in situ composites were investigated. For Al–Ti–Cu system, Cu enhanced the Al–Ti reaction and resulted in the formation of more Al_3Ti particles due to the presence of a small amount of liquid phase during FSP. After FSP, part of Cu was kept in the Al matrix as solute, whereas the other formed Al_2Cu particles. For Al–Ti–Mg system, except for Al_3Ti, some $Ti_2Mg_3Al_{18}$ particles with fine twin lamellas were formed during FSP, resulting in an increase in the total volume fraction of reinforcing particles. Cu and Mg addition increased the strength of the in situ composites substantially due to introduction of more strengthening modes and more reinforcing particles, however the elongation decreased dramatically.

1. Introduction

Aluminide intermetallic particles, such as Al_3Ti, Al_3Ni, and so on, usually exhibit high resistance to wear, high hardness and specific modulus, and good stability at elevated temperature [1]. However, these aluminide particles are usually so brittle that they cannot serve as structural materials directly. Attempts have been made to compensate their brittleness by embedding these particles in the ductile metallic materials, forming aluminide particles reinforced metal matrix composites [2–5].

In the last two decades, in situ aluminide particles reinforced Al matrix composites (AMCs) attracted a wide attention due to their excellent mechanical properties and low density [2–5]. And several in situ techniques such as reactive hot pressing (RHP), mechanical alloying (MA) and exothermic dispersion (XD) have been used to fabricate aluminide particles reinforced AMCs [6–8].

Friction stir processing (FSP), originally developed as a solid-state processing technique for microstructural modification [9], has been also used to fabricate in situ aluminide particles reinforced AMCs by Lee et al. [10,11] and Ke et al. [12], and it was indicated that the in situ aluminide particles reinforced AMCs fabricated via FSP exhibited a good combination of strength and ductility compared with those fabricated via other in situ techniques [10–12]. However these studies [9–12] were all conducted in Al–Me binary systems, thus the reinforcement types are relatively fewer and the strengthening mechanism is less abundant, which limits the further improvement in the mechanical properties of the in situ composites.

The third element addition in the Al–Me binary systems would either act as the alloying element for the Al matrix or form another in situ reinforcement, resulting in additional strengthening to the composites. Furthermore, the third element addition would exert an influence to the in situ reaction process. For example, Brinkman et al. [13] studied the effect of Cu addition on the in situ reaction in an Al–Ti–B system during XD process and suggested that although Cu did not exert a significant effect on the reaction mechanism and phase formation sequence in the Al–Ti–B system, the presence of Cu led to an increase in the reaction rate. Our previous study [14] also suggested that Cu addition accelerated the formation of Al_3Ti in an Al–Ti system during hot pressing at 600 °C due to the presence of Al–Al_2Cu eutectic liquid phase.

In the present study, in situ composites were fabricated using Al–Ti–X(Cu, Mg) systems via FSP, and the aim is to investigate (a) the effect of Cu and Mg addition on the in situ Al–Ti reaction and the formation of Al_3Ti during FSP, (b) the existence state of Cu and Mg in the in situ composites: forming intermetallic particles or being alloying element in the Al matrix, and (c) the effects of Cu and Mg addition on the mechanical properties of the FSP in situ composites.

* Corresponding author. Tel./fax: +86 24 83978908.
E-mail address: zyma@imr.ac.cn (Z.Y. Ma).

0966-9795/$ – see front matter © 2013 Elsevier Ltd. All rights reserved.
http://dx.doi.org/10.1016/j.intermet.2013.04.003

2. Experimental

Three types of in situ composites with nominal compositions of Al-16.4 wt.%Ti, Al-16.4 wt.%Ti-2.5 wt.%Cu and Al-16.4 wt.%Ti-2.5 wt.%Mg, respectively, were fabricated (denoted as Al–Ti, Al–Ti–Cu and Al–Ti–Mg samples, respectively). Commercial pure Al powders (average size 13 μm, 99.9 pct purity), pure Ti powders (average size 45 μm, 99 pct purity), pure Cu powders (average size 18 μm, 99.5 pct purity) and pure Mg powders (average size 32 μm, 99.5 pct purity) were used as raw materials.

The raw powders with the designed compositions were mixed in a bi-axis rotary mixer at a rotation rate of 50 rpm for 12 h and then cold compacted into billets. The cold compacted billets were heated to 500 °C in a vacuum furnace and then hot pressed after being held for 5 min at 500 °C. The hot pressed billets were hot forged at 480 °C into disc plates 10 mm in thickness. The forged plates were subjected to 4-pass FSP with 100 pct overlapping at a tool rotation rate of 2000 rpm and a traverse speed of 25 mm/min. The pin tool was moved along the same line and the subsequent FSP run was applied after the workpiece had been fully cooled from the previous FSP pass. A K-type thermocouple was embedded at the bottom of the stir zone (SZ) to acquire the temperature profiles of the FSP runs. A steel tool with a concave shoulder 20 mm in diameter, a threaded conical pin 8 mm in root diameter, 5.5 mm in tip diameter, and 5.8 mm in length was used for FSP. The tool was made of H13 tool steel with a hardness of HRC 45.

The specimens for microstructural investigations were cut in the transverse direction to the FSP. An X-ray diffraction analyzer (D/max 2400) was used to identify the phases of the composites. The microstructures were examined by scanning electron microscopy (SEM, Quanta 600) with backscattered and secondary electron imaging patterns (BEI and SEI), and transmission electron microscopy (TEM, TECNAI20). The volume fractions of un-reacted Ti particles in various samples were analyzed by the image analysis software (Image-Pro Plus 6.0) from at least 5 SEM images. Thin foils for TEM were prepared by the ion-milling technique. The elemental distribution of the composites was examined by electron probe micro analysis (EPMA-1610).

Dogbone-shaped tensile specimens (5.0 mm gage length, 1.4 mm gage width, and 1.0 mm gage thickness) were electrical discharge machined from the SZ, transverse to the FSP direction. Tensile tests were conducted using an INSTRON 5848 micro-tester at a strain rate of 1×10^{-3} s^{-1}. The property values for each condition were calculated by averaging three test results. After the tensile test, the fracture surfaces of the failed specimens were examined using SEM.

3. Results

Fig. 1(a) shows the XRD patterns of the forged samples. For the three samples, no evident peaks of Al–Ti intermetallics were found, indicating that almost no reaction between Al and Ti took place during hot pressing and forging. For the forged Al–Ti–Cu sample, some peaks corresponding to Al_2Cu were revealed, indicating that Cu reacted with Al during hot pressing and forging. However, for the forged Al–Ti–Mg sample, no evident peaks of Mg-containing intermetallics were found.

Fig. 2 shows SEM/BEI images and the corresponding elemental maps of the forged Al–Ti–Cu and Al–Ti–Mg samples. For the forged Al–Ti–Cu sample, some coarse Cu rich particles were observed, and based on the results of XRD, these particles should be Al_2Cu. Furthermore, it was noted that almost no Cu was distributed in the Al matrix. For the forged Al–Ti–Mg sample, no Mg rich particles were found, and Mg was distributed into the Al matrix, however, the distribution of Mg in the matrix was non-homogeneous.

Fig. 1(b) shows the XRD patterns of the FSP samples. In the three FSP samples, evident peaks of Al_3Ti were found, indicating that Ti reacted with Al to form Al_3Ti during FSP. However, some weak Ti peaks were still detected in the three FSP sample. For the FSP Al–Ti–Cu sample, similar with the forged sample, Al_2Cu peaks were found. For the Al–Ti–Mg sample, except for Al, Al_3Ti and Ti peaks, some peaks corresponding to $Ti_2Mg_3Al_{18}$ were detected, which were absent in the forged Al–Ti–Mg sample.

Fig. 3 shows the SEM/BEI images of the FSP samples. Some fine un-reacted Ti particles (white particles) were observed in the three FSP samples, which is consistent with the XRD results. From image analysis of SEM images, the volume fractions of Ti particles in the FSP Al–Ti, Al–Ti–Cu and Al–Ti–Mg samples are listed in Table 1. It can be seen that less Ti particles remained in the FSP Al–Ti–Cu and Al–Ti–Mg samples than in the FSP Al–Ti sample.

Fig. 4 shows the elemental maps of the FSP Al–Ti–Cu and Al–Ti–Mg samples. In the Al–Ti–Cu sample, some Cu rich particles, with the size much finer than that in the forged sample, could be found, and furthermore, Cu was also distributed into the Al matrix. For the Al–Ti–Mg sample, no evident Mg rich particles were found, and the distribution of Mg in the Al matrix became homogeneous.

Fig. 5 shows the TEM images of the FSP samples. Some rounded Al_3Ti particles with a diameter of ~150 nm were found in all three FSP samples. For the Al–Ti–Cu sample, some Al_2Cu particles with an irregular shape were also revealed, and some fine Al_3Ti particles were often observed in the inner of Al_2Cu particles (Fig. 5(b)). For the Al–Ti–Mg sample, except for Al_3Ti particles, some particles

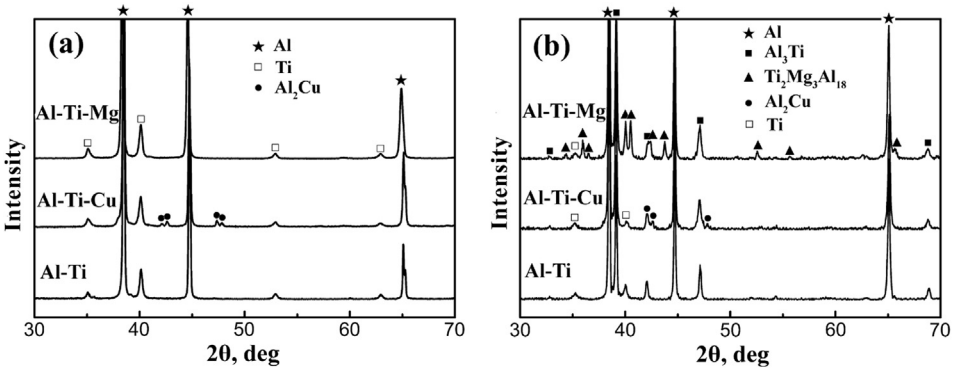

Fig. 1. XRD patterns of (a) forged and (b) FSP samples.

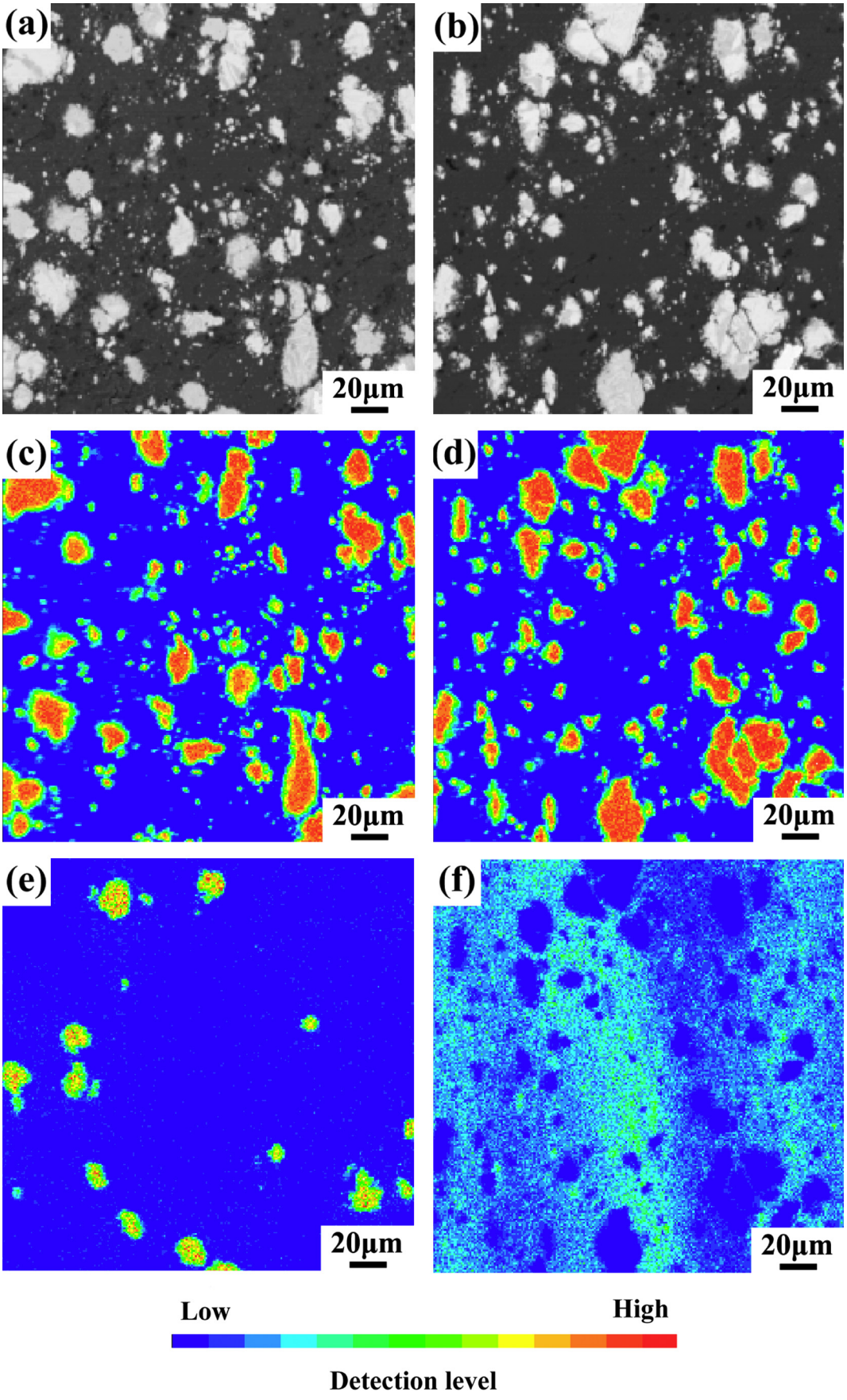

Fig. 2. SEM/BEI images and the corresponding elemental maps of forged samples: (a) Al–Ti–Cu; (b) Al–Ti–Mg; (c) and (e) distribution of Ti and Cu in Al–Ti–Cu sample; (d) and (f) distribution of Ti and Mg in Al–Ti–Mg sample.

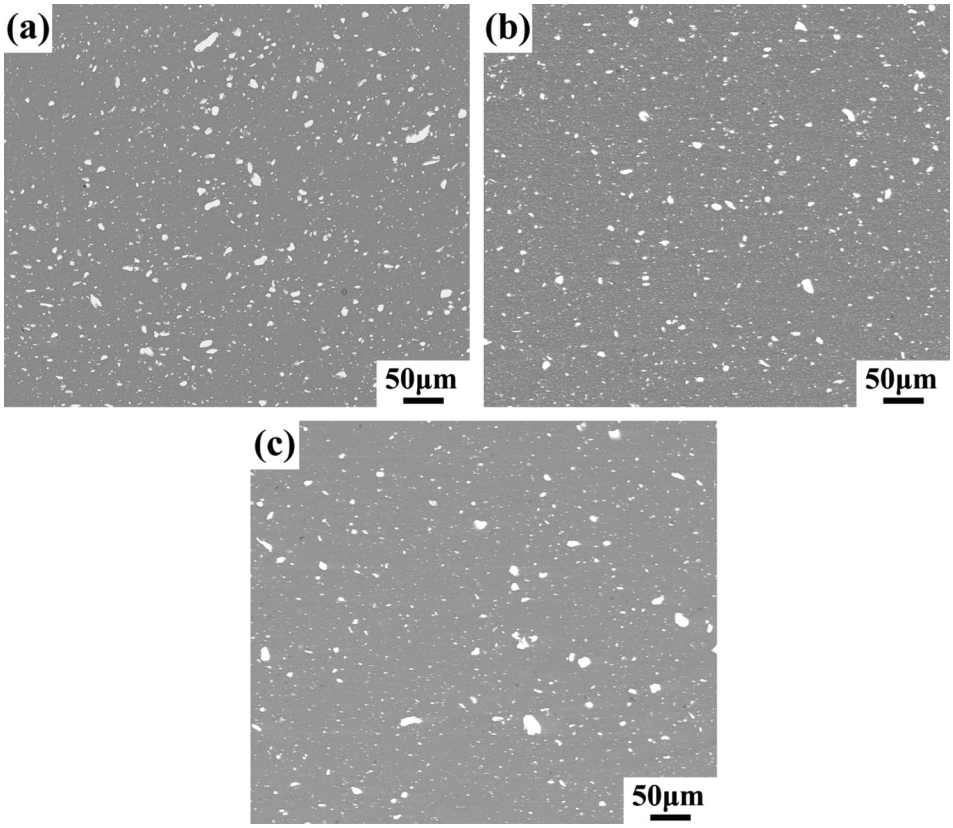

Fig. 3. SEM/BEI images of FSP samples: (a) Al–Ti, (b) Al–Ti–Cu and (c) Al–Ti–Mg.

with fine twin lamellas were detected (Fig. 5(c)). Selected electron diffraction patterns confirmed that these particles are fcc-structured $Ti_2Mg_3Al_{18}$ (Fig. 5(d)).

Fig. 6(a) shows the thermal profiles during FSP of various samples. The peak temperatures of FSP of the Al–Ti, Al–Ti–Cu and Al–Ti–Mg samples are 568 °C, 540 °C and 545 °C, respectively. Considering the measurement error caused by locations of the thermocouples in different samples, it can be concluded that Cu or Mg addition caused little influence on the peak temperature of FSP. Fig. 6(b) shows the DSC curves of various forged samples. Three observations can be made. First, all the DSC curves show an evident endothermic peak at about 660 °C corresponding to the melting of Al matrix. The onset temperature of the melting of Al for the Al–Ti sample is 637 °C, however, it decreased to 612 °C and 623 °C, respectively, for the Al–Ti–Cu and Al–Ti–Mg samples. Second, an exothermic peak was revealed after the melting of Al for the three samples, which should be associated with the exothermic reaction resulting from the formation of different intermetallic particles such as Al_3Ti, $Ti_2Mg_3Al_{18}$. Third, a weak endothermic peak at 546 °C was detected in the curve of the Al–Ti–Cu sample, which should correspond to the eutectic reaction between Al and Al_2Cu, and no evident peak was observed before the melting of Al matrix for the Al–Ti and Al–Ti–Mg samples.

Table 1
Volume fractions of un-reacted Ti and reinforcing particles in FSP samples.

FSP sample	Ti, vol.%[a]	Reinforcing particles, vol.%[b]
Al–Ti	4.6 ± 0.34	29.4 ± 1.2 (Al_3Ti)
Al–Ti–Cu	3.5 ± 0.42	33.3 ± 1.5 (Al_3Ti)
Al–Ti–Mg	3.4 ± 0.23	17.2 (Al_3Ti), 23.8 ($Ti_2Mg_3Al_{18}$)

[a] Experiment values obtained from Fig. 3.
[b] Calculated values.

Fig. 7 shows the engineering stress–strain curves of the FSP samples. The Al–Ti sample exhibited relatively low yield strength (YS, 288 MPa) and ultimate tensile strength (UTS, 371 MPa), and high elongation (18%). For the Al–Ti–Cu sample, the YS and UTS increased to 490 MPa and 678 MPa, while the elongation decreased to 5%. The Al–Ti–Mg sample exhibited a characteristic of brittle fracture with an UTS of 702 MPa and almost negligible elongation.

Fig. 8 shows the SEM fractographs of the FSP samples. Almost no cracked Ti particles were found on the fracture surface of the Al–Ti sample (Fig. 8(a)), and some dimples were observed (Fig. 8(b)). For the Al–Ti–Cu sample, some cracked Ti particles were found (white arrows in Fig. 8(c)), and no obvious dimples were observed in addition to some tearing edges (Fig. 8(d)). The number of cracked Ti particles increased for the Al–Ti–Mg sample (white arrows in Fig. 8(e)), and the fracture surface exhibited a typical pattern of brittle fracture with river pattern (Fig. 8(f)).

4. Discussion

4.1. Formation of intermetallic particles during FSP

For the Al–Ti sample, the Al–Ti reaction did not occur during hot pressing and forging, and subsequent FSP induced the Al–Ti reaction, forming Al_3Ti particles (Fig. 1). This is consistent with our previous study [15,16]. Our previous studies indicated that during FSP, the Al–Ti reaction occurred to form Al_3Ti particles at the Al–Ti interface due to the enhanced Al–Ti interdiffusion and mechanically activated effect caused by severe deformation of FSP, and then the mechanical effect of FSP removed the Al_3Ti particles from the Al–Ti interface and distributed them into matrix uniformly [16].

For the Al–Ti–Cu sample, XRD pattern indicated that Ti did not react with Al in the forged sample, however the Al–Cu reaction

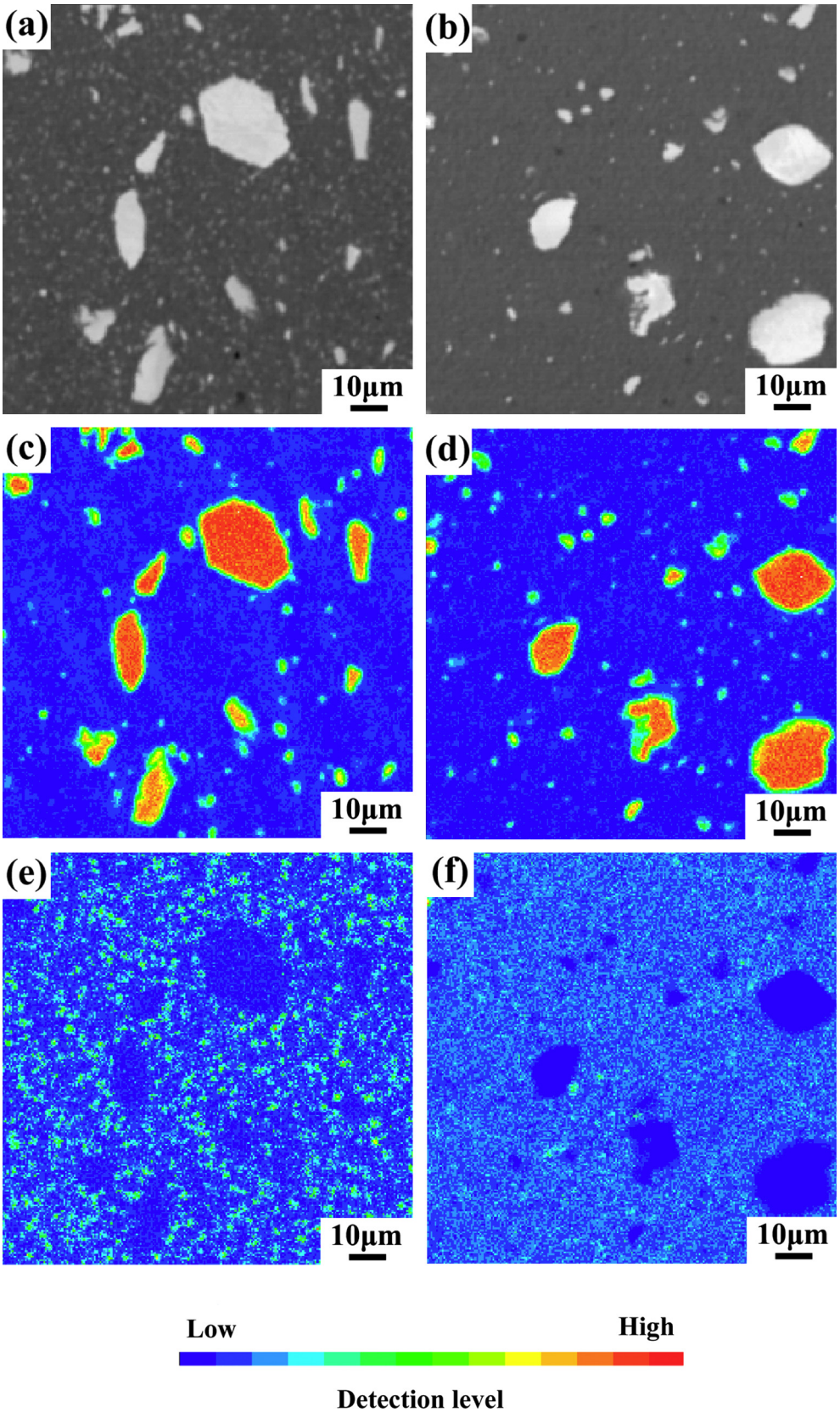

Fig. 4. SEM/BEI images and the corresponding elemental maps of FSPed samples: (a) Al–Ti–Cu; (b) Al–Ti–Mg; (c) and (e) distribution of Ti and Cu in Al–Ti–Cu sample; (d) and (f) distribution of Ti and Mg in Al–Ti–Mg sample.

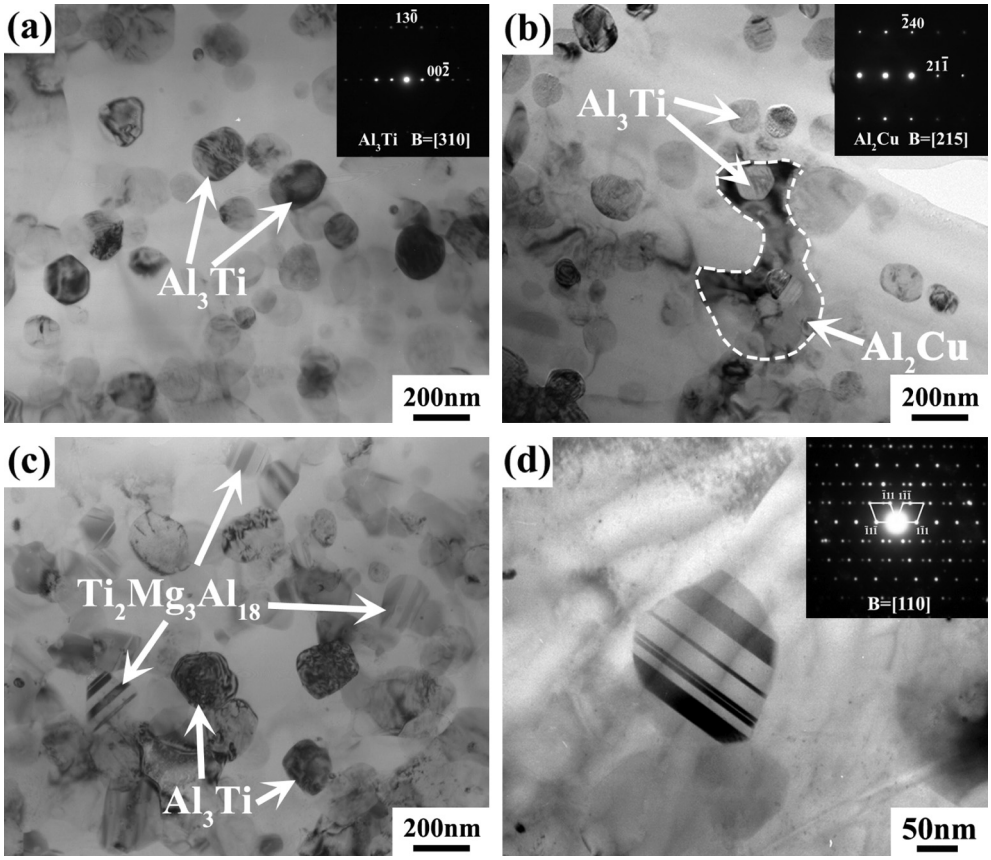

Fig. 5. TEM images of FSP samples: (a) Al–Ti, (b) Al–Ti–Cu, (c) Al–Ti–Mg and (d) $Ti_2Mg_3Al_{18}$ in Al–Ti–Mg sample.

took place to form Al_2Cu during hot pressing and forging due to the high reactive activity of Cu in Al (Fig. 1(a)). During subsequent FSP, the Al–Ti reaction was induced to form Al_3Ti (Fig. 1(b)), which is similar with the situation in the Al–Ti sample. Because, except for Al_3Ti, no other Ti-containing intermetallic particles were detected in the FSP Al–Ti and Al–Ti–Cu samples (Fig. 1), thus in the Al–Ti and Al–Ti–Cu samples, the volume fractions of Al_3Ti can be calculated from the volume fraction of un-reacted Ti in these two samples according to the following reaction formula:

$$3Al + Ti \rightarrow Al_3Ti \quad (1)$$

Based on Eq. (1), the volume fractions of Al_3Ti in the FSP Al–Ti and Al–Ti–Cu samples were calculated to be 29.4% and 33.3%, respectively (Table 1). This fact suggested that Cu addition enhanced the Al–Ti reaction during FSP and resulted in the formation of more Al_3Ti particles.

It is known that melting does not usually occur during FSP due to the self-limiting nature of the process [17]. However, Robson et al. [18] suggested, for cast AZ91 Mg alloy, the partial melting would occur due to its heterogeneous microstructure and low eutectic temperature (~432 °C). In the present study, the results of SEM and elemental maps indicated there were some coarse Al_2Cu particles in the forged Al–Ti–Cu sample (Fig. 2(e)). And the results of DSC also indicated that eutectic reaction between Al and Al_2Cu occurred when the temperature reached 546 °C (Fig. 6(b)). The reaction formula is as follows:

$$Al + Al_2Cu \Leftrightarrow \text{liquid} \quad (2)$$

As shown in Fig. 6(a), the peak temperature near the SZ reached about 550 °C during FSP, which is higher than the temperature of Al–Al_2Cu eutectic reaction. Thus it is expected that some liquid phase with eutectic composition (Al 55.9 wt.%, Cu 44.1 wt.%) would

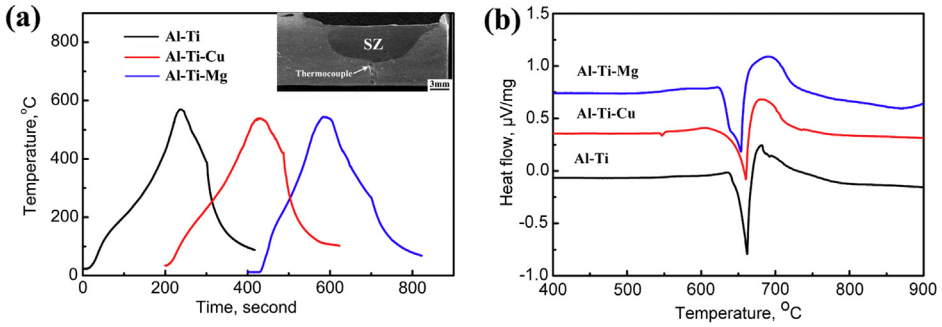

Fig. 6. (a) Thermal profiles during FSP and (b) DSC curves of forged samples.

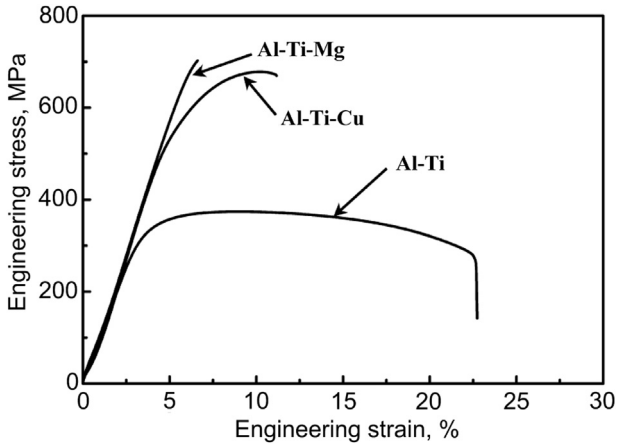

Fig. 7. Tensile curves of FSP samples.

appear during FSP. The Al–Ti interdiffusion between Ti and the liquid phase would occur and the diffusion coefficient would be much higher than that at solid-state [19]. Thus the Al–Ti reaction was enhanced and more Al_3Ti formed during FSP for the Al–Ti–Cu sample.

Robson et al. [18] studied the partial melting during FSP of AZ91 castings and suggested that as the material approached the rotating pin and started to be heavily deformed, it had contained a small fraction of liquid phase. And under the subsequent severe deformation condition produced by FSP, the liquid phase would be stretched and thinned between the heavily sheared solid. This would lead to a very large surface area of liquid and greatly accelerate the transfer of solute between β-phase and Mg matrix [18]. In the present study, similar process would occur and the presence of liquid would facilitate the Al–Ti interdiffusion between Ti and the liquid phase.

As presented above, the Al–Cu eutectic contained 44.1 wt.%Cu, so the presence of the liquid phase would accelerate the diffusion of Cu from Al_2Cu to the Al matrix [20] and then the dissolution of Al_2Cu would also be enhanced. Thus, some Al_2Cu particles would re-precipitate and coarsen during the cooling after FSP [14]. And fine Al_3Ti particles formed during FSP would act the nucleation site of Al_2Cu, so some fine Al_3Ti particles were often observed in the inner of Al_2Cu particles (Fig. 5(b)). Furthermore, part of Cu was retained in solution in the Al matrix because of higher cooling rate compared with furnace cooling.

For the forged Al–Ti–Mg sample, the result of XRD and elemental maps show that no Mg-containing intermetallics formed and Mg was dissolved into the Al matrix, although its distribution was non-uniform (Figs. 1 and 2). This can be attributed to the low temperature of eutectic reaction in the Al–Mg system. According to the Al–Mg diagram and the previous study about sintering of powder mixture of Al and Mg powders, the eutectic liquid appears at 450 °C [21], which is lower than the hot pressing temperature in the present study. As mentioned above, the appearance of liquid would accelerate the diffusion of alloying element, so Mg was dissolved into the Al matrix after hot pressing and forging. However, the holding time during hot pressing was relatively short, thus the distribution of Mg was non-uniform (Fig. 2(f)).

Because Mg was dissolved into the Al matrix in the forged sample, based on the Al–Mg diagram, the liquid phase should appear in the Al solid solution containing 2.5 wt.%Mg at about 620 °C, which is proved by the DSC result in Fig. 6(b), and this temperature is much higher than the peak temperature of the SZ during FSP of the Al–Mg–Ti sample (Fig. 6(a)). Thus it is reasonable to expect that no liquid phase would appear during FSP of the Al–Mg–Ti sample. However, the volume fraction of un-reacted Ti particles in the FSP Al–Ti–Mg sample is much less than that in the FSP Al–Ti sample (Table 1). This is attributed to the formation of $Ti_2Mg_3Al_{18}$ phase in the Al–Ti–Mg sample.

Kerimov et al. [22] studied the reactive diffusion between pure Ti and Al–Mg alloy containing 6–8 at.% Mg at 527–547 °C, and found that except for $Ti_2Mg_3Al_{18}$, no other compound, such as Al_3Ti, Mg_2Al_3, formed at the interface of diffusion couple, indicating that Al_3Ti is not the intermediate product during the formation of $Ti_2Mg_3Al_{18}$. Kerimov et al. [23] suggested that $Ti_2Mg_3Al_{18}$ may have more negative free formation energy than other compound in the Al–Ti–Mg system. Kimura et al. [24] studied the friction welding between Ti–6Al–4V and 5052Al (Al-2.5 wt.%Mg), and also found that only $Ti_2Mg_3Al_{18}$ layer formed at the welded interface. Based on the above analysis, in the present study, $Ti_2Mg_3Al_{18}$ would form preferentially during FSP of the Al–Ti–Mg sample according to the following formula:

$$18Al + 2Ti + 3Mg \rightarrow Ti_2Mg_3Al_{18} \quad (3)$$

and then Al_3Ti formed after the free Mg atoms were consumed almost. In this case, the volume fraction of $Ti_2Mg_3Al_{18}$ and Al_3Ti were calculated to be 23.8% and 17.2%, respectively (Table 1). Thus the total volume fraction of reinforcing particles in the FSP Al–Ti–Mg sample reached 41.0%, which is much higher than that in the FSP Al–Ti and Al–Ti–Cu samples.

In the study of Kerimov et al. [22], $Ti_2Mg_3Al_{18}$ layer with a thickness of 1–3 mm formed in a diffusion couple of pure Ti and Al–Mg alloy after annealed at 547 °C for 1.8×10^6 s. In contrast, a considerable amount of $Ti_2Mg_3Al_{18}$ particles formed in several seconds during FSP (Figs. 1(b) and 5(c)). This fact demonstrated that severe deformation caused by FSP would exert mechanically activated effect on the reaction and therefore accelerate reaction rate significantly. In a previous study, the present authors [16] adopted effective temperature (T_{eff}) to show the mechanically activated effect of severe deformation of FSP on the reaction and suggested the T_{eff} can exceed the melting point of Al during FSP. That is to say, the reaction in severely deformed Al is similar with that in molten Al, so the reaction rate would be significantly enhanced during FSP.

However, some fine twin lamellas were found in the $Ti_2Mg_3Al_{18}$ particles (Fig. 5(d)). The formation of twin lamellas may be associated with severe deformation during FSP and intrinsic properties of $Ti_2Mg_3Al_{18}$, such as stacking fault energy (SFE). In the previous studies, although $Ti_2Mg_3Al_{18}$ was found at the diffusion interface between pure Ti and Al–Mg alloy [22,23] or friction welded interface between Ti–6Al–4V and 5052Al (Al-2.5 wt.%Mg) [24], the internal microstructure of $Ti_2Mg_2Al_{18}$ was not reported.

Recently, Xue et al. [25] reported that FSP can introduce abundant twin lamellas into ultrafined Cu–Al alloys with lower SFE. They [25] suggested that the twin lamellas formed during the recrystallization and grain growth processes of FSP, and can be classified as annealing twins. However, no date about SFE of $Ti_2Mg_3Al_{18}$ was available in the previous literatures. Furthermore, some growth twins can also be introduced in ultrafined Cu grains produced by pulsed electrodeposition [26]. In the present study, the question whether the twins were formed simultaneously with the formation of the $Ti_2Mg_3Al_{18}$ particles or introduced by severe deformation of FSP after the formation of $Ti_2Mg_3Al_{18}$ particles still needs further research.

4.2. Tensile properties and fracture behavior

Fig. 7 shows that, compared with the FSP Al–Ti sample, the strength of the FSP Al–Ti–Cu sample increased substantially, while the elongation decreased to 5%. This is attributed to the following

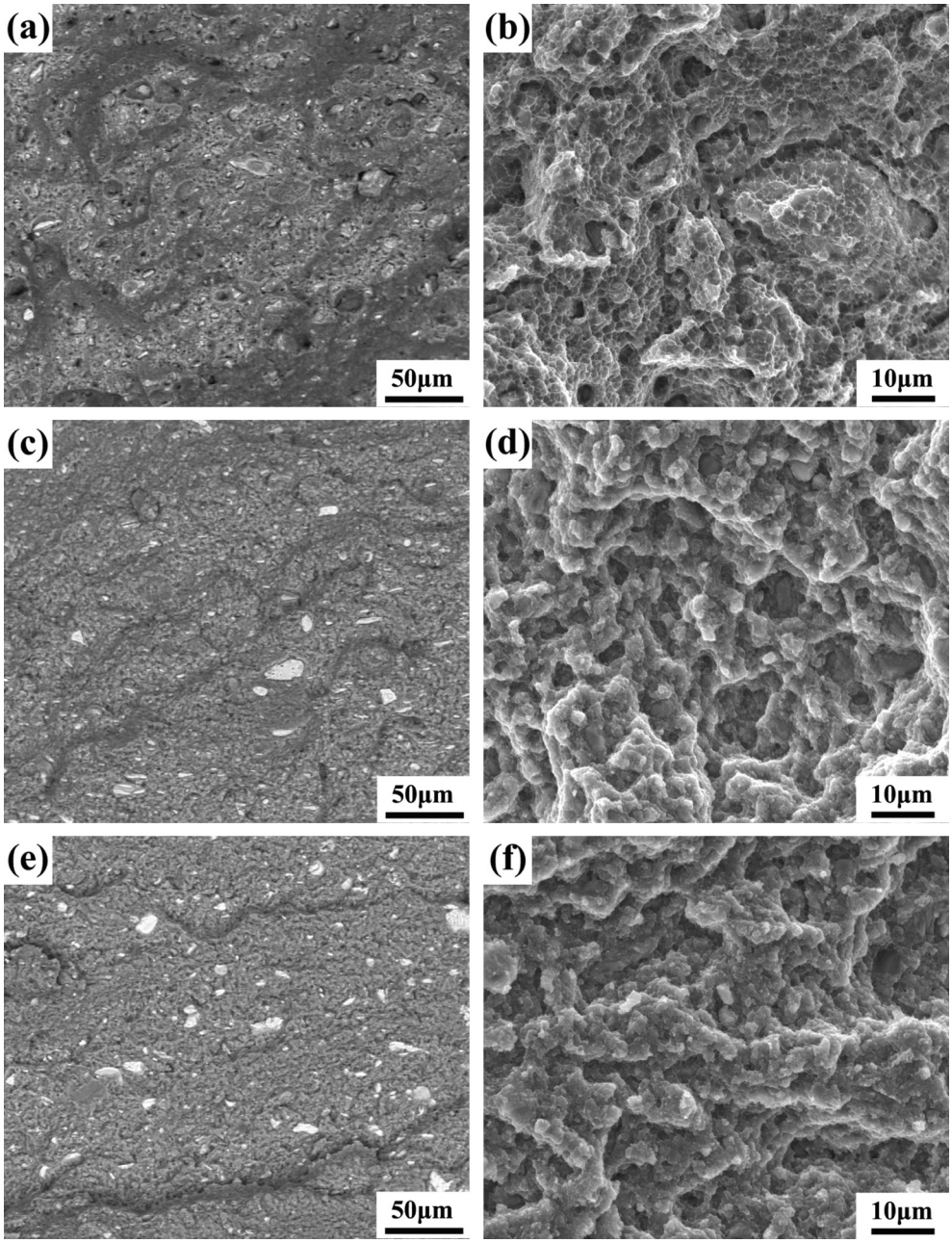

Fig. 8. SEM images of fractures surfaces of FSP samples: (a) Al–Ti (BEI), (b) Al–Ti (SEI), (c) Al–Ti–Cu (BEI), (d) Al–Ti–Cu (SEI), (e) Al–Ti–Mg (BEI), (f) Al–Ti–Mg (SEI).

factors. First, as discussed above, Cu addition enhanced the Al–Ti reaction during FSP, resulting in the formation of more Al_3Ti particles in the Al–Ti–Cu sample. Table 1 shows that the volume fraction of Al_3Ti increased from 29.4% to 33.3% by Cu addition. This would exert more significant strengthening on the matrix through Orowan bowing mechanism. Second, part of Cu was kept in the Al matrix as solute, which would exert additional strengthening effect due to solution strengthening mechanism (Fig. 4(e)). Third, there were some fine Ti particles in the FSP Al–Ti–Cu sample (Fig. 3(b)). The strengthening of the matrix resulted in more efficient load transferring form the matrix to the Ti particles during tension [27]. The fact that more cracked Ti particles were observed on the fracture surface of the FSP Al–Ti–Cu sample than that of the FSP Al–Ti sample confirmed this viewpoint (Fig. 8(c)). Although some Al_2Cu particles precipitated in the FSP Al–Ti–Cu sample, these particles exhibited relatively coarse size, similar with that in over-aged Al–Cu alloy [28], and therefore did not exert obvious strengthening effect on the Al matrix.

For the FSP Al–Ti–Mg sample, the total volume fraction of reinforcing particles ($Al_3Ti + Ti_2Mg_3Al_{18}$) reached to 41% (Table 1). The high volume fraction and the fine size of the reinforcing particles resulted in the smaller interparticle distance, and therefore produced larger strengthening effect on the matrix. The strengthening of the matrix caused more Ti particles to crack during tension (Fig. 8(e)) based on the load transferring mechanism. However, the small interparticles distance also restrained the deformation of the matrix severely [29], resulting in brittle fracture of the FSP Al–Ti–Mg sample (Fig. 8(f)).

Lu et al. [30] and Xue et al. [25] suggested introducing nanosized twin lamellas into ultrafine-grained metal would increase the strength and ductility simultaneously, because twin boundaries not only can effectively resist dislocation motion like conventional grain

boundaries, but also act as slip planes, thus accommodating dislocations. However, in the present study, the fine twin lamellas in the FSP Al–Ti–Mg sample were located in the reinforcing particles, rather than in the matrix. They cannot interact with dislocations directly during tension, so the elongation cannot be improved due to the existence of the fine twin lamellas in the $Ti_2Mg_3Al_{18}$.

5. Conclusions

In summary, in situ Al composites reinforced by various intermetallic particles were fabricated using the Al–Ti–X(Cu, Mg) systems through hot pressing, forging and subsequent FSP, and the formation mechanism of intermetallic particles during FSP and the tensile properties of FSP in situ composites were discussed. The following conclusions can be reached:

1) During hot pressing and forging, the Al–Ti reaction did not take place in the Al–Ti, Al–Ti–Mg and Al–Ti–Cu samples, while Cu reacted with Al to form Al_2Cu in the Al–Ti–Cu sample and Mg dissolved into the Al matrix in the Al–Ti–Mg sample. Subsequent 4-pass FSP induced the Al–Ti reaction in the three samples.
2) For the Al–Ti–Cu sample, Cu enhanced the Al–Ti reaction and resulted in formation of more Al_3Ti particles due to the presence of a small amount of liquid phase during FSP. Al_2Cu experienced dissolution and precipitation during FSP, and part of Cu was kept in the Al matrix as solute after FSP.
3) For the Al–Ti–Mg sample, except for Al_3Ti, some $Ti_2Mg_3Al_{18}$ particles with fine twin lamellas were formed during FSP, resulting in an increase in the total volume fraction of reinforcing particles. The rapid formation of $Ti_2Mg_3Al_{18}$ during FSP can be attributed to the mechanically activated effect of FSP.
4) Cu and Mg addition increased the strength of the in situ composites substantially due to introduction of more strengthening modes and more reinforcing particles, however the elongation decreased dramatically.

Acknowledgments

The authors gratefully acknowledge the support of the National Basic Research Program of China under grant no. 2012CB619600 and the National Natural Science Foundation of China under grant no. 50890171.

References

[1] Rajan TPD, Pillai RM, Pai BC. J Alloys Compd 2008;453:L4–7.
[2] Roy D, Ghosh S, Basumallick A, Basu B. J Alloys Compd 2007;436:107–11.
[3] Ma ZY, Tjong SC. Metall Mater Trans A 1997;28:1931–42.
[4] Srinivasan S, Chen SR, Schwarz RB. Mater Sci Eng A 1992;153:691–5.
[5] Wang SH, Kao PW. Acta Mater 1998;46:2675–82.
[6] Chianeh VA, Hosseini HRM, Nofar M. J Alloys Compd 2009;473:127–32.
[7] Das K, Narnaware LK. Mater Charact 2009;60:808–16.
[8] Varin RA. Metall Mater Trans A 2002;33:193–201.
[9] Mishra RS, Mahoney MW, Mcfadden SX, Mara NA, Mukherjee AK. Scripta Mater 2000;42:163–8.
[10] Lee IS, Kao PK, Ho NJ. Intermetallics 2008;16:1101–8.
[11] Lee IS, Kao PK, Chang CP, Ho NJ. Intermetallics 2013;35:9–14.
[12] Ke LM, Huang CP, Li X, Huang KH. J Alloys Compd 2010;503:494–9.
[13] Brinkman HJ, Duszczyk J, Katgerman L. Mater Sci Technol 1998;14:873–6.
[14] Zhang Q, Xiao BL, Xue P, Ma ZY. Mater Chem Phys 2012;134:294–301.
[15] Zhang Q, Xiao BL, Wang D, Ma ZY. Mater Chem Phys 2011;130:1107–9.
[16] Zhang Q, Xiao BL, Ma ZY. Mater Chem Phys 2013;139:596–602.
[17] Schmidt HB, Hattel JH. Scripta Mater 2008;58:332–7.
[18] Robson JD, Cui S, Chen ZW. Mater Sci Eng A 2012;527:7299–304.
[19] Peng HX, Wang DZ, Geng L, Yao CK. Scripta Mater 1997;37:199–204.
[20] Zhang Q, Xiao BL, Liu ZY, Ma ZY. J Mater Sci 2011;46:6783–93.
[21] Schaffer GB, Sercombe TB, Lumley RN. Mater Chem Phys 2001;67:85–91.
[22] Kerimov KM, Dunaev SF, Sljusarenko EM. J Less-common Met 1987;133:297–302.
[23] Kerimov KM, Dunaev SF. J Less-common Met 1989;153:267–73.
[24] Kimura M, Nakamura S, Kusaka M, Seo K, Fuji A. Sci Technol Weld Joining 2005;10:666–72.
[25] Xue P, Xiao BL, Ma ZY. Scripta Mater 2013;68:751–4.
[26] Lu L, Shen Y, Chen X, Qian L, Lu K. Science 2004;304:422–6.
[27] Nardone VC, Prewo KM. Scripta Mater 1986;20:43–8.
[28] Mondolfo LF. London: Butterworth & Co Ltd.; 1976.
[29] Srivatsan TS, Meslet AH, Smith C, Petraroli M. Mater Sci Eng A 2003;346:91–100.
[30] Lu K, Lu L, Suresh S. Science 2009;324:349–52.